The IRM Quarterly
Fall 1998, Vol. 8, No. 3 Institute for Rock Magnetism

Inside...

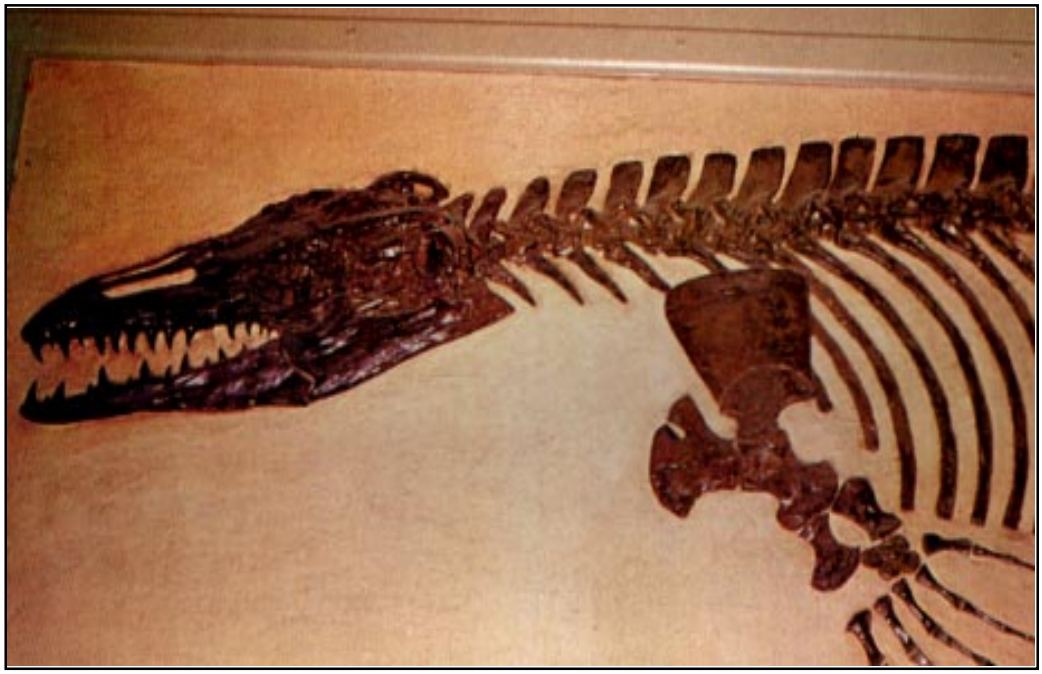

from *The Illustrated Encyclopedia of Dinosaurs*, by D. Norman, Salamander Books Ltd, 1985.

The "business end" of a late Cretaceous Mosasaur, close relative of the modern monitor lizard, and easily more photogenic than our spectrometer.

Mössbauer Revisited

Peter A Solheid
IRM

A new grant from the National Science Foundation and the University of Minnesota will soon allow us to upgrade our second Mössbauer spectrometer, giving us the ability to measure at temperatures down to 4 K and (potentially) in fields up to 5 Tesla.

In the fall 1992 issue of the IRM Quarterly (Vol. 2 No. 3), Chris Hunt explained the basics of Mössbauer spectroscopy and outlined some potential geological applications. Here I will briefly summarize the sort of information that Mössbauer spectroscopy can tell us about iron minerals, and show some examples of data measured at *IRM*. For a more detailed read, please reach for your Fall 1992 issue or one of the references following this article. What!? You don't save all your back issues? Well, no worries, you can point your browser towards our Web site and download a fresh PDF copy!

Basis of Mössbauer Spectroscopy

In 1957 Rudolph Mössbauer discovered what has since become known as the Mössbauer effect. While working as a graduate student in Munich, Mössbauer noted the temperature dependence of the absorption cross section of Ir^{191}. This led him to discover the phenomenon of recoil-free nuclear resonance fluorescence. When a free nucleus (as in a gas) emits a photon, some of the energy of the photon will be lost as the nucleus recoils, resulting in an undeterminable photon energy. However for a nucleus in a solid, the entire mass may absorb the recoil, resulting in negligible photon energy loss. The situation is similar to the difference between throwing a ball while standing on a skateboard (which will allow you to recoil) and throwing a ball while standing on the moon (which will not).

Of the 88 gamma-ray transmissions in which the Mössbauer effect has been detected, there are about 12 for which useful applications have been found. These include iron, tin, gold, antimony, tellurium, iodine, xenon, europium, and neptunium. Fortunately for us, iron is an ideal element for Mössbauer spectroscopy.

Recoil-free photons

An excited state of Fe^{57} at 136.32 keV is produced by electron capture from Co^{57}. About 10% of the transitions from the I = 3/2 excited state to the I = 1/2 ground state of the Fe^{57} nuclei will emit a 14.4 keV gamma ray. Depending on the physical properties of the solid, a certain fraction of these will be recoil-free and are, hence, useful for Mössbauer spectroscopy. Since the nucleus-electron interactions we wish to study shift the energy of absorption of the photons, we need to scan the gamma-beam energy over the range of interest. This is done by moving the source relative to the sample, creating a Doppler shift in the energy of the photons. A velocity of 1 mm/s towards the sample results in an increase of 4.8×10^{-8} eV (14.4keV x v/c). By moving the sample at a constant acceleration to a maximum velocity of ± 10 mm/s or so, we can vary the energy enough to study the effects of nucleus-electron interactions on the absorption of photons by the Fe^{57} in the sample.

These interactions affect the absorption energy in several measurable ways. Below is a brief description of the physical basis, as well as an illustration of how these interactions are manifest in the spectrum. Again a more detailed description can be found in the references at the end of this article.

Isomer shift

A chemical isomer shift is caused by electrostatic interactions between the nucleus and its electrons. This is due to the nucleus being 0.1% larger in the I = 3/2 excited state than in the I = 1/2 ground state. This causes the Mössbauer transition energy to depend on the electron density at the nucleus. Isomer shifts are measured relative to the centroid of a room-temperature iron spectrum and are essentially independent of temperature.

Quadrupole splitting

Any nucleus with a spin quantum number greater than I = ½ has a non-spherical charge distribution, which if expanded as a series of multipoles contains a quadrupole term. The sign depends on the shape of the deformation. A negative quadrupole moment indicates that the nucleus is oblate or flattened along the spin axis, whereas for a positive moment it is prolate or elongate.

Mössbauer

continued on page 6...

Visiting Fellows' Reports

Spring and summer brought a brief and welcome respite from snow and ice, and also brought a host of brief and welcome research visits from Fellows including **Horst-Ulrich Worm**, working on the superparamagnetic-to-stable-single-domain transition; **Beatriz Ortega-Guerrero,** studying the paleo-environmental history of the Sonoran Desert, and, **Zhichun Jing**, investigating the archeology and landscape history of the North China Plain.

Hysteresis Properties of Oceanic Gabbros and the Superparamagnetism of the Yucca Mountain Tuff

Horst-Ulrich Worm
University of Göttingen
huworm@t-online.de

During ODP Leg 176, at the end of last year, the already famous Hole 735B in the southwest Indian Ocean was deepened by another kilometer to a total depth of 1500 mbsf into oceanic layer 3. The gabbros posses high NRM intensities (on average > 2 A/m) and the NRM is of high stability during demagnetization. One key question is to what depth and temperature can the gabbros preserve their primary remanence. Therefore thermoviscous experiments are planned that measure the decay of the primary remanence and the acquisition of secondary components as a function of time and temperature. At the IRM I measured hysteresis loops at room temperature on bulk samples with the old-but-good MacroVSM and loops at temperatures up to Tc on small chips with the ingenious MicroVSM. Hysteresis parameters indicate PSD behavior and on first inspection it seems that the coercivity, for example, decreases rather slowly with increasing temperature. But definite conclusions will have to await further analysis.

The second 'leg' of my stay at the IRM is carved out of superparamagnetic Yucca Mountain Tuff. One phenomenon associated with superparamagnetic grains is the frequency dependence of susceptibility χ_{fd}. Measurements on a large number of natural samples appear to indicate an upper limit of χ_{fd}=15%. However no such upper limit exists in theory. So one nagging question has been whether our theoretical understanding is insufficient, or whether we have just lacked the ideal superparamagnetic samples. Well, it is neither. As I can say now, the theory is OK, and the ideal samples do exist, though their complete magnetic characterization was missing. Thanks to IRM, the latter was completed for three Yucca Mountain Tuff samples containing different narrow distributions of SP grains. The magnetic characterization comprises thermal demagnetization of a low-temperature remanence, hysteresis measurements at low and elevated temperatures, and frequency- and temperature-dependent measurements of susceptibility. Using the obtained coercivity values, it is straightforward to calculate volume distributions from the thermal unblocking curve. The volume distribution is then used to calculate theoretical χ(T) curves for various frequencies, and these are then compared to the experimental results. Agreement is excellent. Figure 1 illustrates how the susceptibility of the YMT with the smallest grain size varies with frequency and temperature. It is apparent that some extremely fine SP samples may very well lack a frequency dependence at room temperature, so the sometimes-drawn conclusion that $\chi_{fd=0}$ implies no SP fraction is generally not justifiable. Figure 2 finally displays the threshold-breaking world record (?) strong frequency dependence of susceptibility for sample CS 914.

PS. Wondering why Yucca Mountain samples are labelled CS? Charley Schlinger gave me these samples ten years ago. (Does anyone know his present address?)

Visiting Fellow Reports

continued on p. 6

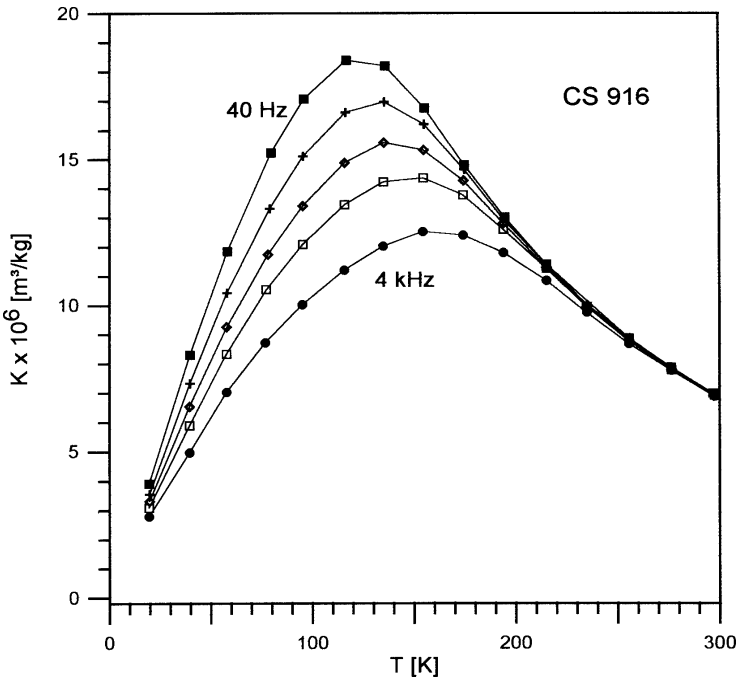

Fig. 1: Frequency and temperature dependence of susceptibility for Yucca Mountain Tuff sample CS916, containing SP grains of approx 10 nm size.

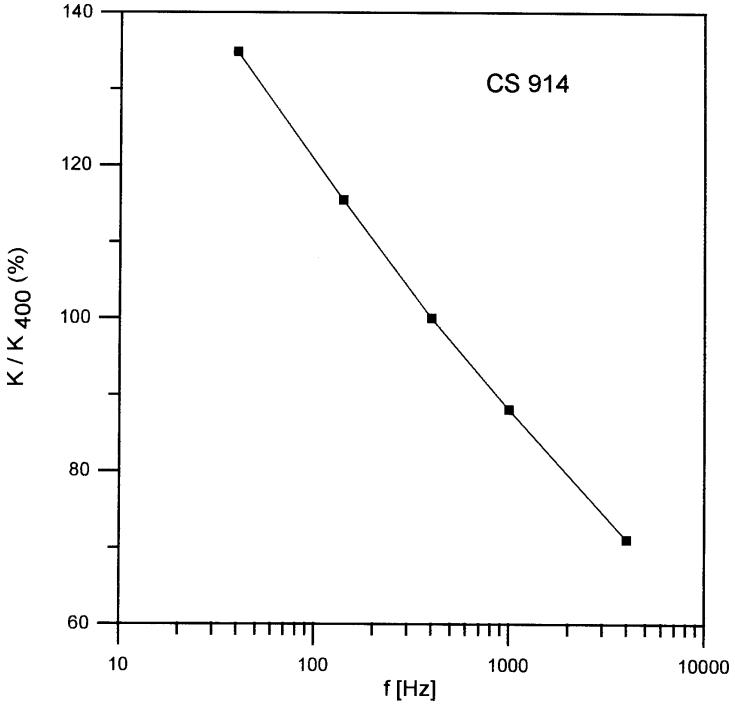

Fig. 2: Frequency dependence of susceptibility at room temperature for sample CS914, with SP grains around 18 nm in size.

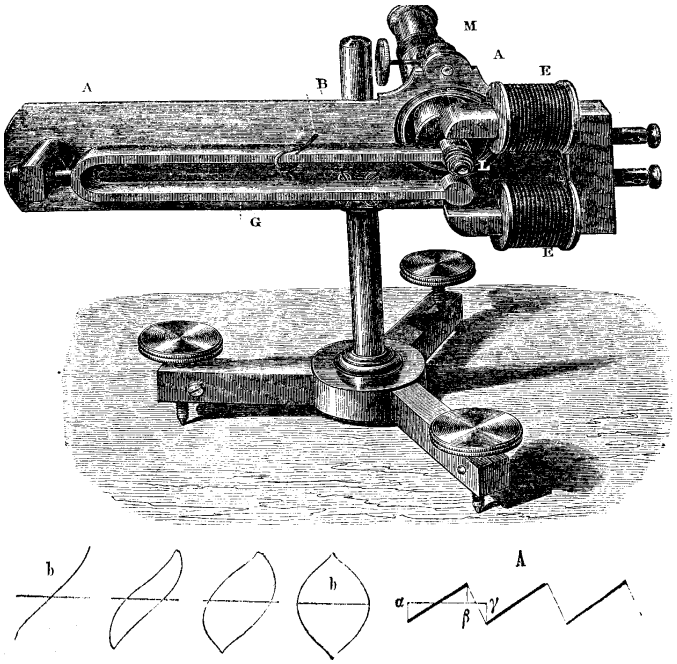

"By applying a peculiar method of observation, proposed in its essential features by the French physicist Lissajous, I have found it possible to observe the vibrational form of individual points on a violin string, and from this observed form, ...to calculate the whole motion of the string and the intensity of the upper partial tones... This instrument may be called a vibration microscope." The lens L is mounted on the end of a tuning fork kept in constant sinusoidal vibration by the electromagnet E; the violin string is marked at a point and bowed so as to oscillate in a direction perpendicular to the vibrations of the fork. The superposed orthogonal motions generate Lissajous figures for the point, and Helmholtz thereby calculated the sawtooth vibration of the string. [On the Sensations of Tone as a Physiological Basis for the Theory of Music, by Hermann Helmholtz, trans. by Alexander J Ellis, Dover, 1954.]

Current Abstracts

A list of current research articles dealing with various topics in the physics and chemistry of magnetism is a regular feature of the IRM Quarterly. *Articles published in familiar geology and geophysics journals are included; special emphasis is given to current articles from physics, chemistry, and materials-science journals. Most abstracts are culled from* INSPEC *(© Institution of Electrical Engineers),* Geophysical Abstracts in Press *(© American Geophysical Union), and* The Earth and Planetary Express *(© Elsevier Science Publishers, B.V.), after which they are subjected to Procrustean editing and condensation for this newsletter. An extensive reference list of articles (primarily about rock magnetism, the physics and chemistry of magnetism, and some paleomagnetism) is continually updated at the* IRM. *This list, with more than 4200 references, is available free of charge. Your contributions both to the list and to the Abstracts section of the* IRM Quarterly *are always welcome.*

Instrumentation

C. Rossel, M. Willemin, A. Gasser, H. Bothuizen, G. I. Meijer and H. Keller, 1998, **Torsion cantilever as magnetic torque sensor**: *Review of Scientific Instruments, v. 69,* p. 3199-203.
A macroscopic cantilever for capacitive torque magnetometry has been developed and tested. It is based on torsion arms in order to obtain better damping against external vibrations than with ordinary cantilevers of similar size. Calibrations yield a torque sensitivity better than $5*10^{-13}$ Nm under optimized conditions. This device can also be used to detect magnetic fields down to 10 nT.

Magnetic Microscopy and Spectroscopy

N. K. Menon and J. Yuan, 1997, **Identification of orientation of magnetic moments in hematite (α-Fe_2O_3) using linear dichroism in spatially resolved EELS in STEM**: *Electron Microscopy and Analysis, v. 1997,* p. 281-4.
We demonstrate the effect of magnetic linear dichroism (MLD) in electron energy loss spectroscopy (EELS), as applied to α-Fe_2O_3. The experiments were performed in a high resolution scanning transmission electron microscope (STEM), capable of producing a nanoscale electron probe. The resultant difference spectrum compares well with theoretical simulations of MLD and with known magnetic structure of hematite. This suggests that MLD in EELS, coupled with the high spatial resolution attainable in STEM, is a useful technique in the study of magnetic microstructure.

S. Music, G. P. Santana, G. Smit and V. K. Garg, 1998, **^{57}Fe Mössbauer, FT-IR and TEM investigations of Fe-oxide powders obtained from concentrated $FeCl_3$ solutions**: *Journal of Alloys and Compounds, v. 278,* p. 291-301.
The chemical and microstructural properties of oxide phases precipitated from concentrated $FeCl_3$ solutions were investigated using ^{57}Fe Mössbauer spectroscopy, Fourier transform infrared spectroscopy and transmission electron microscopy. The initial pH of the precipitation system determined the mechanism of phase transformations. TEM observation showed that the particle size and morphology of the oxide phases were very dependent on the experimental parameters.

Micromagnetic Modeling

K. Fukuma and D. Dunlop, 1998, **Grain-size dependence of two-dimensional micromagnetic structures for pseudo-single-domain magnetite (0.2-2.5 μm)**: *Geophysical Journal International, v. 134,* p. 843-8.
For saturation remanence states, Monte Carlo modelling produced vortex structures for small PSD grains (≤0.25 μm) and closure domain structures for larger PSD grains (0.6-2.5 μm). Between 0.25 and 0.6 μm, structures remained chaotic even after a very large number of Monte Carlo steps. In grains with a closure domain structure, domain walls were usually subdivided into several segments with opposite polarities of magnetization rotation.

Paleoclimate and Magnetic Proxy Records

R. W. Barendregt, J. S. Vincent, E. Irving and J. Baker, 1998, **Magnetostratigraphy of Quaternary and late Tertiary sediments on Banks Island, Canadian Arctic Archipelago**: *Canadian Journal of Earth Sciences, v. 35,* p. 147-61.
Sediments approximately 50 m thick from Banks Island contain one of the longest terrestrial records of Pleistocene climate changes in North America. In the Matuyama Reversed Zone, there are at least two and possibly as many as five full continental glaciations and interglacials, and a preglacial interval. The Brunhes Normal Zone records three full continental glaciations and interglaciations. The Brunhes-Matuyama boundary occurs within interglacial deposits. The first continental glaciation in the western Canadian Arctic postdated the first glaciation in the Canadian Cordillera (2.6 Ma) by at least a million years.

C. Colin, C. Kissel, D. Blamart and L. Turpin, 1998, **Magnetic properties of sediments in the Bay of Bengal and the Andaman Sea: impact of rapid North Atlantic Ocean climatic events on the strength of the Indian monsoon**: *Earth and Planetary Science Letters, v. 160,* p. 623-35.
Magnetic grain-size variations have a strong 23 kyr periodicity, with smaller grain sizes during periods characterized by a strong summer monsoon; Heinrich events and cold stadial events are characterized by relatively large magnetic grain sizes. Furthermore, Heinrich events are characterized by lower values of the chemical index of alteration, implying significantly drier conditions on the continent. The authors suggest that North Atlantic Heinrich events are related to weaker summer monsoon over the Himalaya via an atmospheric teleconnection.

Z. Rixiang, R. S. Coe, G. Bin, R. Anderson and Z. Xixi, 1998, **Inconsistent palaeomagnetic recording of the Blake event in Chinese loess related to sedimentary environment**: *Geophysical Journal International, v. 134,* p. 867-75.
Palaeomagnetic records suggest a threefold subdivision of the Chinese loess plateau into (1) the central and southern regions east of the Liupan Mountains, where the record of the Blake event has been wiped out by pedogenic processes; (2) the northern margin of the loess plateau to the east of the Liupan Mountains, where frequent, severe dust storms have resulted in discontinuous records with a high probability of missing the Blake event; and (3) the region west of the Liupan Mountains, where loess sequences are deposited rapidly and nearly continuously with only minor pedogenesis, and are thus capable of recording short events like the Blake.

L. Sagnotti, F. Florindo, K. L. Verosub, G. S.

Abstracts
continued on p. 4

Wilson and A. P. Roberts, 1998, **Environmental magnetic record of Antarctic palaeoclimate from Eocene/Oligocene glaciomarine sediments, Victoria Land Basin**: *Geophysical Journal International, v. 134*, p. 653-62.
Magnetic susceptibility, intensity of natural and artificial remanences, hysteresis parameters and magnetic anisotropy of the lower half of the CIROS-1 core reveal alternating intervals of high and low magnetic mineral concentrations that do not correspond to lithostratigraphic units in the core, but match changes in clay mineralogy. Weathering processes and input of detrital PSD magnetite to the Victoria Land Basin were intense during periods when the Antarctic climate was warmer than today. A cold and dry climate was not established in Antarctica until the Eocene/Oligocene boundary, with major ice sheet growth occurring at the early/late Oligocene boundary.

J. S. Stoner, J. E. T. Channell and C. Hillaire-Marcel, 1998, **A 200 ka geomagnetic chronostratigraphy for the Labrador Sea: indirect correlation of the sediment record to SPECMAP**: *Earth and Planetary Science Letters, v. 159*, p. 165-81.
A chronostratigraphic framework for the last 200 ka, based on geomagnetic paleointensity, has been derived for the Labrador Sea. Relative paleointensity records derived from three piston cores are correlated to the Sint-200 paleointensity composite [Guyodo & Valet]. Support for the new chronostratigraphic framework is provided by: (1) consistent correlation of Labrador Sea detrital layers to North Atlantic Heinrich layers; (2) general consistency between planktic $\delta^{18}O$ values and the SPECMAP reference curve; and (3) feasible prediction for the age of ash layer 2.

Paleomagnetic Field Records

J. Carlut and V. Courtillot, 1998, **How complex is the time-averaged geomagnetic field over the past 5 Myr?**: *Geophysical Journal International, v. 134*, p. 527-44.
Formal uncertainties in the Johnson & Constable nonlinear inversion would indicate that there are significant nonzonal terms at least up to degree and order 4. Using a compilation of two different data sets from lavas (0 to 5 Ma) and the Johnson & Constable codes, we test the robustness of this result. The data set has been divided into three subsets: the Brunhes polarity data (B), all normal polarity data (N) and all reverse data (R). In each subset of data, a prominent g_2^0, of the order of 5 per cent of g_1^0, is clearly present, as previously established by several authors. Because of limitations in resolution, it may not yet be possible to identify robustly terms other than the axial dipole and quadrupole. The persistence of high-latitude flux concentrations, hemispheric asymmetry or normal versus reversed field asymmetry cannot yet be considered as demonstrated.

J. E. T. Channell, D. A. Hodell, J. McManus and B. Lehman, 1998, **Orbital modulation of the Earth's magnetic field intensity**: *Nature, v. 394*, p. 464-8.
We report a spectral analysis of sedimentary records of relative geomagnetic palaeointensity from two North Atlantic sites which shows significant power both at orbital eccentricity (100 kyr) and obliquity (41 kyr). The eccentricity power is also present in bulk magnetic properties (such as susceptibility) and is therefore attributable to lithological variations controlled by eccentricity-driven climate change. The obliquity power, however, is not apparent in bulk magnetic properties, and seems to be a property of the geomagnetic field itself, thus providing evidence for the orbital forcing of geomagnetic field intensity.

A. A. Kosterov and M. Prevot, 1998, **Possible mechanisms causing failure of Thellier palaeointensity experiments in some basalts**: *Geophysical Journal International, v. 134*, p. 554-72.
The normally magnetized zone of the Jurassic Lesotho basalts shows anomalous Thellier behaviour: typically the slope of the NRM-TRM curves is very steep at intermediate temperatures (200 to 400-460° C). Measurements between room temperature and the Curie temperature show some irreversible changes in hysteresis characteristics. The loss of a fraction of the NRM at temperatures apparently lower than the blocking temperatures in nature may result from the reorganization of the domain structure of the PSD grains during heating. This transformation, which seems to be triggered by the coercivity decrease at very moderate temperatures, can reduce the NRM intensity without requiring any correlated pTRM acquisition.

C. G. Constable, L. Tauxe and R. L. Parker, 1998, **Analysis of 11 Myr of geomagnetic intensity variation**: *Journal of Geophysical Research, v. 103*, p. 17735-48.
Spectral analysis shows that the relative intensity record from Site 522 in the South Atlantic is minimally influenced by climate variations. Isothermal remanence is the most effective normalizer for these data, although both susceptibility and anhysteretic remanence are also adequate. Paleointensity variations follow a gamma distribution and are compatible with predictions from modified paleosecular variation models and global absolute paleointensity data. When subdivided by polarity interval the variability in paleointensity is proportional to the average, and the average is weakly correlated with interval length.

D. V. Kent and M. A. Smethurst, 1998, **Shallow bias of paleomagnetic inclinations in the Paleozoic and Precambrian**: *Earth and Planetary Science Letters, v. 160*, p. 391-402.
Anomalously shallow inclination distributions for the Paleozoic and Precambrian can be explained by a geomagnetic field source model which includes a relatively modest contribution (25% of the axial dipole) from a zonal octupole field and an arbitrary zonal quadrupolar contribution. The apparent change by around 250 Ma to a much more axial dipolar field geometry might be due to stabilization of the geodynamo by growth of the inner core. Alternatively, the anomalous inclination distributions may reflect a tendency of continental lithosphere to be cycled into the equatorial belt, perhaps because geoid highs associated with long-term continental aggregates influence true polar wander.

D. N. Thomas, T. C. Rolph, J. Shaw, S. Gonzalez de Sherwood and Z. Zhuang, 1998, **Palaeointensity studies of a late Permian lava succession from Guizhou Province, south China: implications for post-Kiaman dipole field behaviour**: *Geophysical Journal International, v. 134*, p. 856-66.
Biostratigraphic dating of interbedded limestone units and stratigraphic constraints indicate an age close to the termination of the Kiaman reverse superchron. The normal polarity characteristic remanence held by the lavas implies a post-Kiaman age for this succession. Thellier palaeointensity results from the lavas indicate comparatively low dipole field strength shortly after the termination of the superchron. 80% of samples yield VDM values in the range 42-52% of the present-day value. This suggests that a low-energy dipole existed at least between 300 and 255 Ma and does not appear to have been confined to the stable reverse polarity interval.

Synthesis and Properties of Magnetic Minerals

Y. Q. Cai, M. Ritter, W. Weiss and A. M. Bradshaw, 1998, **Valence-band structure of epitaxially grown Fe_3O_4(111) films**: *Physical Review B, v. 58*, p. 5043-51.
Well-ordered Fe_3O_4 (111) films prepared epitaxially on clean Pt(111) surfaces are chemically identical to bulk single crystals. We have studied the electronic structure of such an ordered Fe_3O_4 (111) film using angle-resolved photoemission in conjunction with synchrotron radiation. Subtle differences in the valence-band structure are observed above (at 300 K) and below (at 90 K) the Verwey transition temperature (120 K) , which may be attributed to a structural change and/or a charge ordering associated with the Verwey transition. The resonant behavior shows, however, no temperature dependence, indicating that resonant photoemission in Fe_3O_4 remains a localized process and is not influenced by the Verwey transition.

J. Ding, W. F. Miao, E. Pirault, R. Street and P. G. McCormick, 1998, **Mechanical alloying of iron-hematite powders**: *Journal of Alloys and Compounds, v. 267*, p. 199-204.
Mechanically alloyed $xFe\cdot(1\text{-}x)Fe_2O_3$ powders had a nanocrystalline structure with a particle size of 5-10 nm and consisted of Fe_2O_3 and Fe_3O_4 for $x \leq 0.2$, Fe_3O_4 and FeO for x=0.2-0.5 and FeO and Fe for $x \geq 5.0$. Nanocrystalline metastable FeO decomposed into nanocrystalline Fe_3O_4 and Fe after annealing at 250-400° C and reformed again to submicron FeO after annealing at temperatures above 550° C. Nanocomposites of Fe_3O_4 /Fe obtained by decomposition after annealing at 300° C exhibited high values of magnetisation and coercivity.

M. G. Ferreira da Silva and M. A. Valente, 1998, **Crystallization and properties of sol-gel derived $10Fe_2O_3$-$10Al_2O_3$-$80SiO_2$ glass-ceramics**: *Journal of Non Crystalline Solids, v. 232-234*, p. 409-415.
Iron aluminosilicate samples were prepared by the sol-gel method. X-ray diffraction (XRD),

scanning electron microscopy (SEM) and a.c. susceptibility measurements ($\chi_{a.c.}$) were used to study the role of heat-treatment temperature and atmosphere on magnetite precipitation. The results obtained prove that it is possible to prepare ferrimagnetic glass-ceramics at temperatures less than 1000º C. The amount of magnetite present in the samples depends on the heat-treatment temperature and atmospheric conditions.

M. Field, C. J. Smith, D. D. Awschalom, N. H. Mendelson, E. L. Mayes, S. A. Davis and S. Mann, 1998, **Ordering nanometer-scale magnets using bacterial thread templates**: *Applied Physics Letters, v. 73*, p. 1739-41.
Nanometer-scale ferromagnetic particles (Fe_2O_3, Fe_3O_4) are dispersed within a mutant bacterial chain which is drawn into a macroscopic fiber "rope." Cross-sectional SEM images reveal that the iron oxide particles are intercalated between the walls of the bacterial cells which are bundled into parallel threads. The field-dependent switching is seen to markedly sharpen when the synthesis is conducted within an applied magnetic field.

B. Hannoyer, M. Ristic, S. Popovic, S. Music, F. Petit, B. Foulon and S. Dalipi, 1998, **Ferritization of Ni^{2+} ions in mixed hydroxide suspensions**: *Materials Chemistry and Physics, v. 55*, p. 215-23.
Mixed hydroxide suspensions with a molar ratio of NiO: Fe_2O_3 =1:1 were aged at 25º, 90º or 120º C for various times. Ferritisation of Ni^{2+} ions in these suspensions was studied by analysis of the solid products separated from the mother liquor. The actual phase composition of the samples was very dependent on the experimental conditions. FT-IR spectroscopy and ^{57}Fe Mössbauer spectroscopy indicated Ni^{2+} ferritization at 90º and 120º C, and provided evidence that this process was possible even at 25º C.

E. L. Mayes, F. Vollrath and S. Mann, 1998, **Fabrication of magnetic spider silk and other silk-fiber composites using inorganic nanoparticles**: *Advanced Materials, v. 10*, p. 801-5.
The functionalization of spider silk fibers promises to produce high-strength fibers with very interesting properties, for example, magnetism. A method is described to prepare hybrid spider silk materials by binding inorganic nanoparticles to the surface or near-surface region of a silk fiber immersed in a colloidal sol. Magnetite-silk fiber remains flexible.

Y. Okano and T. Nakamura, 1998, **Hydrothermal synthesis of aluminum bearing magnetite particles**: *Colloids and Surfaces A, v. 139*, p. 279-85.
Aluminum-bearing magnetite particles were synthesized by aerial oxidation of alkaline suspensions containing both ferrous and aluminum ions. From magnetization measurement at low temperature, it was found that most of the aluminum ions in the oxide state were incorporated into the octahedral site.

L. Suber, R. Zysler, A. G. Santiago, D. Fiorani, M. Angiolini, A. Montone and J. L. Dormann, 1998, **Size and shape effect on the magnetic properties of α-Fe_2O_3 nanoparticles**: *Materials Science Forum, v. 5476*, p. 1-7.
The magnetic properties and the Morin transition (T_M=263 K in the bulk system) of α-Fe_2O_3 nanoparticles have been investigated for different size (3-700 nm) and shape (rhombohedral, acicular and spherical), by analyzing the temperature dependence of the zero-field-cooled (ZFC) and field-cooled (FC) magnetization. For rhombohedral (30-350 nm) and spherical (10-50 nm) particles, T_M decreases with decreasing particle size and increasing magnetic field. Acicular particles (350-700 nm) do not show the Morin transition, unless annealed. In samples with a large distribution of particle size, the measurements show the superimposed effects of superparamagnetism and the Morin transition. Only the superparamagnetic component is observed for the smallest spherical particles (3 nm), whose average blocking temperature is about 140 K.

X. G. Wang, W. Weiss, S. K. Shaikhutdinov, M. Ritter, M. Petersen, F. Wagner, R. Schlogl and M. Scheffler, 1998, **The hematite (α-Fe_2O_3) (0001) surface: evidence for domains of distinct chemistry**: *Physical Review Letters, v. 81*, p. 1038-41.
Using spin-density functional theory we investigated various possible structures of the hematite (0001) surface. Depending on the ambient oxygen partial pressure, two geometries are found to be particularly stable under thermal equilibrium, one being terminated by iron and the other by oxygen. Both exhibit huge surface relaxations (-57% for the Fe and -79% for the O termination) with important consequences for the surface electronic and magnetic properties. With scanning tunneling microscopy we observe two different surface terminations coexisting on single crystalline α-Fe_2O_3 (0001) films, which were prepared in high oxygen pressures.

Remanence and Magnetization Processes

Y. Enomoto and Z. Zhong, 1998, **Possible evidences of earthquake lightning accompanying the 1995 Kobe earthquake inferred from the Nojima fault gouge**: *Geophysical Research Letters, v. 25*, p. 2721-4.
The Kobe earthquake of January 17, 1995, which had a magnitude of 7.2, was accompanied by earthquake lightning (EQL). The fault gouge near ground level at the Nojima fault, near where the EQL was witnessed, was highly lithified and anomalously magnetized. The characterization of the fault gouge and the mudstone near the fault suggests that the anomalies might have been induced by an intense EQL current which passed through the fault plane.

C. Papusoi, Jr., A. Stancu, C. Papusoi, J. L. Dormann, M. Nogues and E. Tronc, 1998, **Algorithm for the computation of the FC and ZFC magnetization curves for nanoparticle systems**: *IEEE Transactions on Magnetics, v. 34*, p. 1138-40.
A new model for the FC and ZFC magnetization processes for fine particle systems uses a two-level model for the thermal relaxation. An approximate method for the resolution of the master equation for a temperature or field varying process is developed. The volume and easy axis distributions as well as the temperature dependencies of the intrinsic magnetization and anisotropy are taken into account. Numerical results are in good agreement with experimental data obtained for various concentration γ-Fe_2O_3 nanoparticle systems.

D. V. Dimitrov, G. C. Hadjipanayis, V. Papaefthymiou and A. Simopoulos, 1998, **Surface-induced magnetism in α-Fe_2O_3 /Ag multilayers**: *Journal of Magnetism and Magnetic Materials, v. 188*, p. 8-16.
Anomalous ferromagnetic-like behavior, with significant magnetization and very large coercivities at low temperatures was observed in α-Fe_2O_3 /Ag multilayers. Mössbauer studies showed the presence of two magnetic components, bulk-like and surface-like with substantially lower hyperfine field. The observed magnetic moment per particle can be accounted for by the contribution of only about 5% of the total number of surface Fe^{3+} ions. Large shifts in the hysteresis loops of field-cooled samples indicate strong exchange coupling between the antiferromagnetic core and the net magnetic moments on the surface.

S. L. Halgedahl, 1998, **Revisiting the Lowrie-Fuller test: alternating field demagnetization characteristics of single-domain through multidomain glass-ceramic magnetite**: *Earth and Planetary Science Letters, v. 160*, p. 257-71.
In assemblages of glass-ceramic magnetite with average grain sizes varying from less than 0.1 μm to approximately 100 μm, weak-field TRM and weak-field ARM are in all cases more stable to alternating field demagnetization than is (Jrs). Calculations show that populations of noninteracting, uniaxial SD grains should behave in just the opposite sense to that reported originally by Lowrie and Fuller. This discrepancy could be due to magnetic interactions; however, a second and intriguing explanation of the SD-like results obtained from all samples is that AF demagnetization characteristics reflect a strong dependence of local energy minimum domain state, and its associated stability, on the state of magnetization.

S. Hu, E. Appel, V. Hoffmann, W. W. Schmahl and S. Wang, 1998, **Gyromagnetic remanence acquired by greigite (Fe_3S_4) during static three-axis alternating field demagnetization**: *Geophysical Journal International, v. 134*, p. 831-42.
GRM acquisition is unexpectedly observed during AF demagnetization in about 20% of a large number of samples. X-ray diffraction (XRD) analysis on a magnetic extract clearly shows that greigite is the dominant magnetic mineral carrier. Scanning electron microscopy (SEM) reveals that the greigite particles are in the grain size range of 200-300 nm. Greigite clumps of about 3 μm size are sealed by silicates. GRM is mainly produced perpendicular to the AF direction, but a smaller GRM component was also found along the demagnetization axis.

...continued from page 1

This is one of the most useful interactions for Mössbauer spectroscopy.

Hyperfine field

A third important hyperfine interaction is the nuclear Zeeman effect. This occurs if there is a magnetic field at the nucleus. The field can either be internal due to unpaired electrons or externally applied. The magnetic field splits the nuclear level of spin I into equi-spaced substates. The Mössbauer transition can take place for certain nuclear levels.

Applications

Mössbauer spectroscopy is a powerful tool when used in connection with rock magnetism in order to help characterize a sample. In many cases Mössbauer analysis provides information that is difficult or impossible to obtain through magnetic measurements alone..

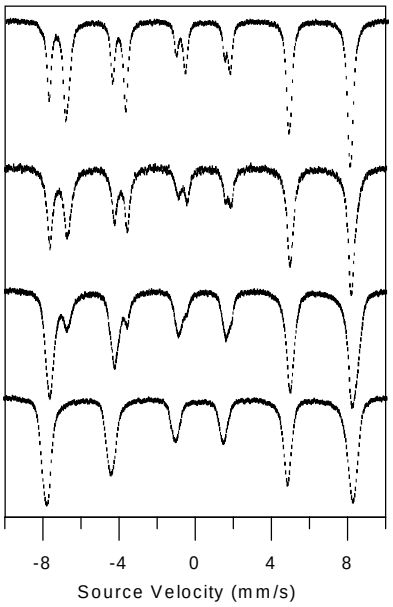

Figure 1. Spectra of synthetic magnetite/ maghemite mixtures (top to bottom: 100/0, 75/25, 25/75, 0/100)

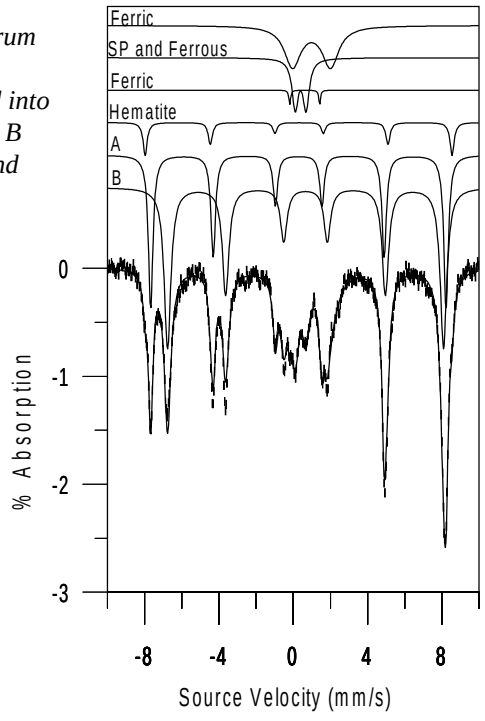

Figure 2. Spectrum of Alaskan loess sample, resolved into magnetite A and B site, hematite, and other mineral components.

Mineralogy

Minerals with similar magnetic properties can be difficult to distinguish using traditional rock magnetic methods. A good example is the determination of mixtures of maghemite and magnetite, or the degree to which magnetite is non-stoichiometric. While magnetite can often be detected by the presence of a Verwey transition or Curie point, maghemite is not as easily detected. There is currently no low-temperature method of positively identifying maghemite, and it often converts to hematite upon heating. Enter Mössbauer spectroscopy. Figure 1 shows spectra of pure magnetite, mixtures of magnetite and maghemite (75-25 and 25-75), and pure maghemite. Note the change in area of the peaks. While the outer peak of magnetite (A site) overlaps with a maghemite peak, the inner peak of magnetite (B-site) does not. Magnetite's B-site contains two Fe atoms, (Fe^{+2}, Fe^{+3}) while the A-site contains only 1 (Fe^{+3}). The ratio of the inner to outer peak area should be 2:1 for pure magnetite. A shift in area from the inner to the outer indicates maghemitization.

Another mineralogical application is analysis of weakly-magnetic iron minerals in the presence of others with very strong magnetizations. For example hematite (J_s = 0.4 Am^2kg^{-1}) is often masked magnetically by even a low concentration (few percent) of magnetite (J_s = 92 Am^2kg^{-1}). In a Mössbauer spectrum, however, all Fe atoms are treated equally, so a sample containing a 50-50 mixture of magnetite-hematite would give distinct spectra with 50% of the area attributable to hematite and 50% attributable to magnetite. Figure 2 shows fits to a spectrum from a magnetic extract of Alaskan loess, showing the presence of magnetite/maghemite, hematite, and other minerals containing ferrous and ferric iron.

Superparamagnetism

Ultra-fine superparamagnetic (SP) grains can often be difficult to characterize using traditional rock-magnetic measurements. Where unblocking temperature and frequency dependence can give information on grain size, it is often not possible to determine the mineralogy of such grains. Mössbauer spectroscopy can give additional information on grain size as well as determine the mineralogy. By cooling a sample that is superparamagnetic at room temperature to below its blocking temperature a distinct characterizable spectrum is obtained. The blocking temperature for Mössbauer measurements is generally higher than for magnetic remanence measurements, because the time for the Mössbauer transition to take place on the nuclear scale is very small, on the order of 10^{-7} seconds. If the relaxation time is longer than this the grain will behave as a stable single-domain (SSD) particle during the measurement. For remanence measurements, in contrast, SSD behavior is related to relaxation times on the order of $10^2 - 10^4$ seconds or longer.

Knowing the measurement time and blocking temperature we can also calculate a grain size distribution with certain assumptions. Using Néel theory and making some assumptions about the anisotropy constant, we can calculate a volume as follows:

$$v = [kTln(tf_0)]K^{-1}$$

where v = volume, T = temperature, k = Boltzmann's constant, t = relaxation time = 10^{-7} seconds, f_0 is the frequency factor = 10^9 seconds, and K is the anisotropy constant. If we assume K is only from magnetocrystalline anisotropy ($1.36x10^5$ $ergs/cm^3$ for magnetite) we can calculate the SP – SSD transition for Mössbauer measurements of magnetite at various temperatures.

Temperature (K)	Diameter (nm)
300	14
200	12
100	10
77	9
50	8
4.2	3.5

Figure 3 (on page 8) illustrates the spectra obtained at various temperatures for a sample of synthetic magnetite with a mean particle diameter of 11 nm. With decreasing temperature, the SP-SSD transition is evident as the sextet becomes more prominent. Also the A and B sites begin to overlap due to suppressed electron hopping.

Additional Resources

There are several sources for more detailed information on Mössbauer Spectroscopy. One of the best references is the book *Mössbauer Spectroscopy* by Greenwood and Gibb, published in 1971 by Chapman and Hall. On the WWW point your browser to the site of the Web Research Company (not web as in www) at http://sluggo.iaxs.net/webresco/ and click on the link to Mössbauer Spectroscopy. On that site you can also find a more comprehensive list of references. In the (near) future we will be adding some data to the IRM's Mössbauer spectrometer page at http://www.geo.umn.edu/orgs/irm/equipment/mossbauer/index.htm.

The Study of Site Formation Processes Using Rock Magnetism

Zhichun Jing
Archaeometry Laboratory
University of Minnesota, Duluth
zjing@d.umn.edu or zjing@ssc.wisc.edu

The nature and origin of the sedimentary matrix is critically important in understanding the formation and development of an archaeological site in its landscape context. Various techniques of rock magnetism have been used to study the sedimentary matrix of archaeological sites by helping address issues relevant to site formation processes. My primary objective at IRM was to measure room-temperature magnetic properties of 400 samples from two archaeological sites, Shangqiu and Anyang, in the North China plain. Shangqiu is traditionally considered the homeland of the Shang civilization (1,750 - 1,100 BC) which is the first literate civilization in China and East Asia. Anyang was the capital for the last twelve kings of the Shang Dynasty (1,300 - 1,100 BC). The Archaeometry Laboratory - UMD has on-going geoarchaeological projects at these two culturally important sites. At both sites the general aim is to study the changing relationships between humans and the land and resources they exploited during prehistoric and early historic periods. Rock magnetic techniques can help achieve the general goal by addressing three specific research subjects: (1) site formation processes, (2) micro- or meso-environmental changes at a site and its environs, particularly local climatic conditions, and (3) culturally induced soil erosion.

At the IRM I first made anhysteretic remanent magnetization (ARM) and low-field magnetic susceptibility (χ) measurements on all 400 samples. Then I used the Princeton Measurements VSM to determine hysteresis properties and S-ratio for 178 selected samples, and the Lakeshore Susceptometer to measure frequency dependence of susceptibility over a wide range of frequencies on 26 selected samples. Using these measured magnetic parameters, one can characterize the magnetic mineral composition, concentration, and grain size.

At Shangqiu two general alluvial units - pre-Neolithic paleosol and historic alluvium - constitute the Holocene stratigraphy, providing both sedimentary and stratigraphic contexts for archaeological sites of different periods. Magnetic properties of the two units differ significantly (the historic alluvium is significantly higher in both *ARM* and χ than the pre-Neolithic paleosol), possibly due to the changes in the hydrological system in the past 2000 years. With the *ARM vs.* χ data for these units we are able to examine the linkage of anthropogenic sediments of different periods to their sediment sources. The presence of a significant superparamagnetic (SP) fractions may complicate the use of *ARM vs.* χ models because SP grains contribute only to χ and not ARM. A specific objective of my visit to the IRM was to investigate the presence of SP particles, by measuring hysteresis loops and frequency dependence of susceptibility.

The samples from Anyang were taken from many different contexts, both cultural and natural. Our geoarchaeological survey has revealed a complex stratigraphic sequence, due to interaction of the fluvial and aeolian processes that have dominated the geomorphic evolution in the Anyang area. Systematic samples from excavation profiles and off-site geological cores were measured at the IRM in order to study processes responsible for the formation of archaeological sites. In addition, my interest for this site was to look at any potential magnetic signals that might indicate climatic changes during prehistoric and early historic periods, and the impacts of human land use on physical landscape, particularly the effects on the regional landscape of the establishment and development of late Shang urban center from the end of 14th century to late 11th century BC.

Definite conclusions will have to await a more careful study of the data obtained from my nine days of stay at the IRM. However it is already clear that magnetic properties are sensitive indicators of the mineralogical and grain-size variations that resulted from changes in the environmental context of these sites.

Magnetic characteristics of a playa lake sediments in Baja California

Beatriz Ortega Guerrero
Universidad Nacional Autonoma de Mexico
bortega@tonatiuh.igeofcu.unam.mx

The extensive paleoclimatic work in the SW North America has generated a number of unresolved questions related to the origin, chronology and extent of climatic change during Late Quaternary in this region. Despite the extensive work done in the US, this research is scarce in the Mexican portion, particularly in western part of the Sonoran Desert. With the aim to investigate the record of climatic and environmental change, we collected sediments from Laguna San Felipe (Baja California), in a 9.5 m long core. This sequence spans the last ca. 60,000 yr. Preliminary results from mineral magnetic and sedimentological analyses showed highly contrasting characteristics between the glacial and the late glacial-Holocene sediments. Late Pleistocene sediments (lower part of the sequence) show very low magnetic concentration values, typically SIRM<1 mAm^2kg^{-1} and χ of 0.05-0.2 mm^3kg^{-1}. The late glacial and Holocene sediments (the sediments younger than ca. 12,000 yr, upper part of the sequence) display a five-fold increase in magnetic concentration, and, apparently, in χ_{fd}%, as measured in the Bartington susceptometer. This remarkable contrast between the Pleistocene and Holocene sediments seen in magnetic parameters is also observed in the loss-on-ignition, mean particle size and sedimentation rates calculated from the available ^{14}C dating.
The objective of my visit to the IRM was to investigate the magnetic carriers in these sediments, and to test the suggested presence of SP grains. ARM results also present the same pattern previously observed in SIRM and χ: it is very low in the lower part of the sequence, ~ 0.01 mAm^2kg^{-1}, and higher in the upper part, up to 0.2 mAm^2kg^{-1}. The thermomagnetic behavior of samples measured in the mVSM from both the lower and the upper part of the sequence, yielded a Curie temperature of 580 ºC. Ratios of hysteresis parameters measured at room temperature, H_{CR}/H_C and M_R/M_S, indicate

VF Reports *continued on page 8...*

von Helmholtz, Hermann

b. Aug. 31, 1821, Potsdam; d. Sept. 8, 1894, Berlin

Helmholtz completed his dissertation at the Friedrich-Wilhelm Institute of Medicine and Surgery in 1842, on ganglia nerve cells. His first important scientific paper, *Über die Erhaltung der Kraft* (1847), was one of the earliest clear statements of the principle of conservation of energy. He made pioneering contributions to the physics and physiology of sight and sound with *Handbook of Physiological Optics* (1856) and *Theory of the Sensations of Tone as a Physiological Basis of the Theory of Music* (1863). Of central importance in potential field theory is Helmholtz's Theorem that a vector field can be uniquely determined from its divergence and curl. He worked on the mathematical basis of electromagnetism, attempting to derive observed phenomena from theoretical conceptions of the ether. A Helmholtz coil system, with circular DC coils separated by a distance equal to their radius, generates a magnetic field with high spatial uniformity near the center of the system.

Mössbauer
...continued from page 6

Figure 2. Spectra of synthetic 11-nm magnetite at various temperatures.

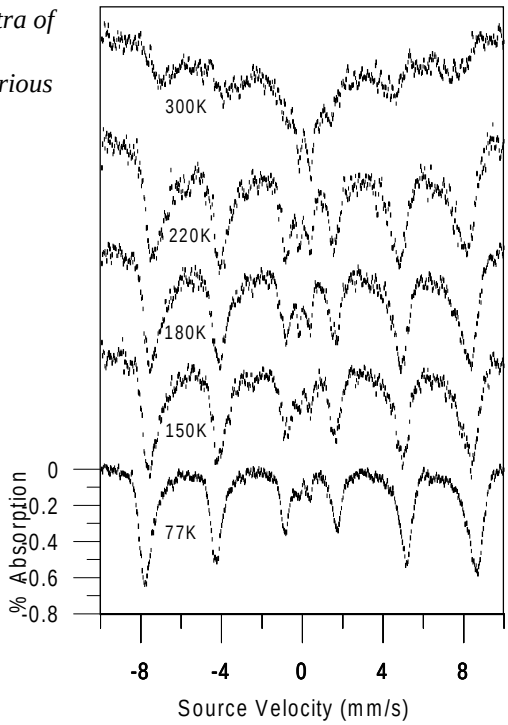

VF Reports
...continued from page 7

the dominance of MD grains in the lower part of the sequence. Samples from the upper part cluster around 2-2.5 of H_{CR}/H_C and 0.15-0.2 of M_R/M_S, plotting in the right lower part of the PSD region in the Day biplot.

After some excitement and fun provided for free to the IRM staff by getting a sample-holder straw stuck in the Lakeshore susceptometer (and making them aware of new ways to do it), I began to test the presence (or absence) of SPM grains. Room temperature measurements of frequency dependent susceptibility showed that, even if $\chi_{fd}\% > 3$ is present in several samples from the lower section, percentages in the upper section are 8.5-12. Temperature variation of susceptibility between 10 and 300 ºK measured in five frequencies, also suggested the presence of SPM grains in the upper section.

Thermal demagnetization of low temperature IRM measured in the Quantum Design MPMS showed the Verwey transition in most of the samples from the lower section, and only in the sandy samples from the upper part. The general decrease of IRM between 10 and 300 ºK in the upper samples also reflect a strong SPM component. Measurements in zero field cooling and field cooling in the same sample failed to reveal magnetite of bacterial origin.

Current analysis of independent proxy records (pollen), chemical analysis on these sediments and magnetic studies in samples from surrounding modern soils, will help us to constrain the possible interpretations (climatic/environmental signal or chemical signal) of the magnetic behavior observed in our samples.

Visiting Fellowship Applications Due Soon

The *IRM*, with its unique array of well-maintained and carefully calibrated instrumentation, is yours for the asking! Applications are due December 15, 1998 for *IRM* Visiting Fellowships during the interval March 1 - August 31, 1999. An *IRM* Visiting Fellowship gives you full access to our laboratory facilities for up to ten days, along with a travel allowance of up to $500 (sorry, per diem expenses - lodging and meals -are not included). *IRM*'s staff will assist you in optimizing your experimental design, in learning to use each instrument, and in interpreting measured data. You also get as much lab coffee as you can tolerate.

All you have to do to apply is to write a brief (2-3 page) proposal describing the experiments or measurements you want to carry out, and their significance. Applications are welcome from researchers in any country and in any field of study relevant to the magnetism of natural materials. In general, advanced studies with specific, well-defined objectives, and which make effective use of the *IRM*'s unique instrumentation, are given preference over initial reconnaissance studies, or investigations based on "routine" measurements (i.e., using widely-available equipment). However, we also recognize the value of some more exploratory research. We expect to award seven Visiting Fellowships for the spring-summer interval.

Get an official cover page and instrument scheduling worksheet from our Web site, or request one by mail, and return it by December 15, 1998.

Collector's Series #11

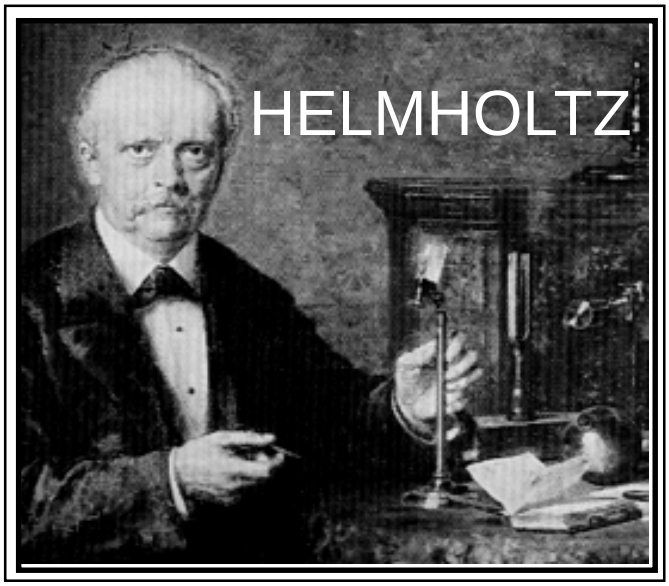

from *Hermann von Helmholtz*, by Helmut Rechenberg, 1994, VCH Verlagsgesellschaft

The *Institute for Rock Magnetism* is dedicated to providing state-of-the-art facilities and technical expertise free of charge to any interested researcher who applies and is accepted as a Visiting Fellow. Short proposals are accepted semi-annually in spring and fall for work to be done in a 10-day period during the following half year. Shorter, less formal visits are arranged on an individual basis through the Facilities Manager.

The *IRM* staff consists of **Subir Banerjee**, Professor/Director; **Bruce Moskowitz**, Associate Professor/Associate Director; **Jim Marvin**, Senior Scientist; **Mike Jackson**, Senior Scientist and Facility Manager, and **Peat Solheid**, Scientist.

Funding for the *IRM* is provided by the **W. M. Keck Foundation**, the **National Science Foundation**, and the UofM.

The *IRM Quarterly* is published four times a year by the staff of the *IRM*. If you or someone you know would like to be on our mailing list, if you have something you would like to contribute (*e.g.*, titles plus abstracts of papers in press), or if you have any suggestions to improve the newsletter, please notify the editor:

Mike Jackson
Institute for Rock Magnetism
University of Minnesota
291 Shepherd Laboratories
100 Union Street S. E.
Minneapolis, MN 55455-0128
phone: (612) 624-5274
fax: (612) 625-7502
e-mail: irm@geolab.geo.umn.edu
www.geo.umn.edu/orgs/irm/irm.html

I R M

Institute for Rock Magnetism